2017

A TRANSFER MATRIX APPROACH TO DETERMINE THE LOW FREQUENCY INSERTION LOSS OF ENCLOSURES INCLUDING APPLICATIONS

Shujian He
University of Kentucky, she227@g.uky.edu
Digital Object Identifier: https://doi.org/10.13023/ETD.2017.472

STUDENT AGREEMENT:

I represent that my thesis or dissertation and abstract are my original work. Proper attribution has been given to all outside sources. I understand that I am solely responsible for obtaining any needed copyright permissions. I have obtained needed written permission statement(s) from the owner(s) of each third-party copyrighted matter to be included in my work, allowing electronic distribution (if such use is not permitted by the fair use doctrine) which will be submitted to UKnowledge as Additional File.

I hereby grant to The University of Kentucky and its agents the irrevocable, non-exclusive, and royalty-free license to archive and make accessible my work in whole or in part in all forms of media, now or hereafter known. I agree that the document mentioned above may be made available immediately for worldwide access unless an embargo applies.

I retain all other ownership rights to the copyright of my work. I also retain the right to use in future works (such as articles or books) all or part of my work. I understand that I am free to register the copyright to my work.

REVIEW, APPROVAL AND ACCEPTANCE

The document mentioned above has been reviewed and accepted by the student's advisor, on behalf of the advisory committee, and by the Director of Graduate Studies (DGS), on behalf of the program; we verify that this is the final, approved version of the student's thesis including all changes required by the advisory committee. The undersigned agree to abide by the statements above.

Shujian He, Student

Dr. D. W. Herrin, Major Professor

Dr. Haluk E. Karaca, Director of Graduate Studies

A TRANSFER MATRIX APPROACH TO DETERMINE THE LOW FREQUENCY INSERTION LOSS OF ENCLOSURES INCLUDING APPLICATIONS

THESIS

A Thesis submitted in partial fulfillment of the

requirements for the degree of Master of Science

in Mechanical Engineering in the College of Engineering

at the University of Kentucky

By

Shujian He

Lexington, Kentucky

Director: Dr. Herrin, Professor of Mechanical Engineering

Lexington, Kentucky

2017

ABSTRACT OF THESIS

A TRANSFER MATRIX APPROACH TO DETERMINE THE LOW FREQUENCY INSERTION LOSS OF ENCLOSURES INCLUDING APPLICATIONS

Partial enclosures are commonly used to reduce machinery noise. However, it is well known in industry that enclosures sometimes amplify the sound at low frequencies due to strong acoustic resonances compromising the performance. These noise issues are preventable if predicted prior to prototyping and production. Though boundary and finite element approaches can be used to accurately predict partial enclosure insertion loss, modifications to the model require time for remeshing and solving. In this work, partial enclosure performance at low frequencies is simulated using a plane wave transfer matrix approach. Models can be constructed and the effect of design modifications can be predicted rapidly. Results are compared to finite element analysis and measurement with good agreement. The approach is then used to design and place resonators into a sample enclosure. Improvements in enclosure performance are predicted using plane wave simulation, compared with acoustic finite element analysis, and then validated via measurement.

KEYWORDS: Partial Enclosures, Plane Wave Simulation, Insertion Loss, Finite Element Method, Acoustic Resonator, Passive Noise Control.

Shujian He

Student's Signature

11th December, 2017

A TRANSFER MATRIX APPROACH TO DETERMINE THE LOW FREQUENCY INSERTION LOSS OF ENCLOSURES INCLUDING APPLICATIONS

By

Shujian He

Dr. Haluk E. Karaca

Director of Graduate Studies

Dr. D. W. Herrin

Director of Thesis

11th December, 2017

Date

ACKNOWLEDGEMENTS

Firstly, I would like to express my great appreciation to my advisor Professor D. W. Herrin for his precious guidance and patient help during my study at the University of Kentucky. He has been playing a tremendous role in my career. I do thank Professor Tingwen Wu as well for his help and advice during my studies and research. In addition, my great thanks also go to Dr. John Baker for his wonderful support and valuable advice. I would like to express my appreciation to my friends in the Vibro-Acoustics group: Wanlu Li, Huangxing Chen, Jundong Li, Gong Cheng, Yitian Zhang, Kangping Ruan, Keyu Chen, Peng Wang, Ruimeng Wu, Weiyun Liu, Shishuo Sun, Caoyang Li, Nan Zhang, Jonathan Chen, Xin Hua, Limin Zhou, Jinghao Liu, Jiawei Liu, Conner Campbell and Rui He, for all the priceless help in the past several years, and for every fun moment we had together. I also want to precise my thanks to my family. I cannot express how grateful I am to my father Laifei He and mother li Guo for all the support and sacrifices.

TABLE OF CONTENTS

LIST OF FIGURES

LIST OF TABLES

CHAPTER 1 INTRODUCTION

1.1 Introduction

Noise from rotating machinery is an ever-present annoyance in daily life. It is present whether driving, riding, flying, at work, or at home. Rotating machinery includes diesel and internal combustion engines, motors, pumps, compressors, and fans. High machinery noise levels can degrade hearing and human health over time. Moreover, product sales can be adversely affected if the noise is unacceptable or even noticeable. In the automotive industry, the sound of the vehicle directly impacts sales and is one of the more noticeable characteristics to the customer.

Due to increasing concerns about noise, engineers regularly implement countermeasures in a vehicle or other product. Perhaps the best way to reduce the noise is to decrease the noise at the source. This may be accomplished by reducing running forces. For example, fan noise can be decreased by lowering the speed and using larger blades to insure the same total flow. Engine ignition timing can be optimized so that the combustion process is smoother and even. Nonetheless, sources must still produce a certain amount of power and accompanying noise.

If the source cannot be changes, modifications can also be made to the path to reduce noise levels. This includes structurally isolating a source using compliant mounts or acoustically isolating a source by adding mufflers, sound

absorption, or enclosures. Mufflers are commonly added to the intake or exhaust to attenuate combustion and supercharger noise. For sound radiation from machinery, enclosures are commonly used to reduce the noise levels at the receiver. An enclosure is essentially a small room with sound absorption placed on the walls

Enclosures may be full or partial. Full enclosures have no openings and the dominant transmission path is from the air space inside the enclosure, into the walls, and then from the walls to the receiver. In that case, the enclosure should function well so long as it is properly isolated from the source and the enclosure walls are sufficiently massive. Partial enclosures are more commonly used but the effectiveness is compromised by the openings which are the primary path of sound propagation. Openings cannot be avoided due to flow and thermal considerations.

Partial enclosures are widely used in industry to reduce noise emissions from generator sets, refrigeration units, HVAC equipment, and other machinery. Enclosure walls are normally made from metal or plastic and are sufficiently massive to negate transmission through the walls. The primary acoustic path of interest is through the enclosure openings.

Acoustic enclosures are usually lined with sound absorbing materials which provide substantial noise reduction at the middle and high frequencies where sound absorption is effective. Simple formulas can be used to approximate the enclosure performance at these frequencies. The amount of enclosure attenuation

primarily depends on the size of the openings, amount of sound absorptive coverage, and the effectiveness of the sound absorption.

However, the sound absorption is ineffective at the lower frequencies and enclosures often amplify the source at the low frequency resonances of the enclosed space. If the machinery operates at or close to a low frequency enclosure resonance, it can be anticipated that the enclosure will be ineffective and may even increase the noise. If this occurs, the product will likely be unacceptable and the noise issue will need to be mitigated. Resonant issues are commonly dealt with by insuring that the prime mover does not operate at the acoustic resonant frequencies, or by adding resonators to the enclosure to reduce the noise.

At the present time, most problems which arise are dealt with on an ad hoc basis. Some designers use boundary or finite element analysis to determine the enclosure resonant frequencies. However, analyses require substantial amounts of time to prepare a mesh and then solve the model. If changes to the enclosure are considered, a new mesh must be generated and solved. Hence, numerical simulation is primarily used as a virtual prototyping tool rather than as a virtual design tool.

In the current work, a simplified plane wave approach is used to identify low frequency enclosure resonances. Partial enclosures can be modeled quickly and solutions with useable accuracy can be performed in seconds. Moreover, the approach is conducive to providing the designer with a better intuitive understanding of how to modify the enclosure to improve the acoustic performance.

The plane wave simulation approach is validated using acoustic finite element analysis and via measurement.

After the simplified plane wave approach is laid out, the method is then used to introduce resonators into the enclosure tested. Resonators include quarter wave tubes and Helmholtz resonator arrays. It is shown that the added resonators can improve the enclosure performance by up to 20 dB at selected frequencies.

1.2 Objectives

The objectives of this research are to:

1. Develop a simplified plane wave methodology to determine the insertion loss of a partial enclosure.
2. Validate the plane wave approach using finite element analysis and direct measurement.
3. Use the plane wave approach to design enclosures with resonators to eliminate resonance issues. Resonators considered include an enclosure with a quarter wave tube and with Helmholtz resonator arrays.

1.3 Outlines

This chapter has served to introduce the need for research in the topic and the objectives of the research.

Chapter 2 provides background on the problem. Enclosure metrics, analytical and numerical simulation approaches, and some theoretical background are surveyed. In chapter 3, two models are used to validate the plane wave

approach by comparing to direct measurement and the finite element method. Chapter 4 looks at introducing resonators o identify and treat low frequency enclosure resonances. The plane wave simulation approach introduced in Chapter 3 proves very beneficial as a virtual design tool. Chapter 5 summarizes the work and recommends follow on research.

CHAPTER 2 BACKGROUND

2.1 Insertion Loss

The metric that is most commonly used to assess the performance of an enclosure is the sound power insertion loss (IL_W) defined as the difference between the sound power level radiated by the unenclosed source (L_{WO}) to that with the enclosure (L_{WE}). Insertion loss can be expressed mathematically as

$$IL_W = L_{WO} - L_{WE} \tag{2-1}$$

where L_{WO} and L_{WE} are expressed in dB. The sound power is most easily measured by sound intensity scanning or the reverberation room method. The difference in sound power can also be approximated by comparing sound pressure level measurements in the far field without and with the enclosure. Throughout this work, insertion loss is used to quantify the enclosure performance.

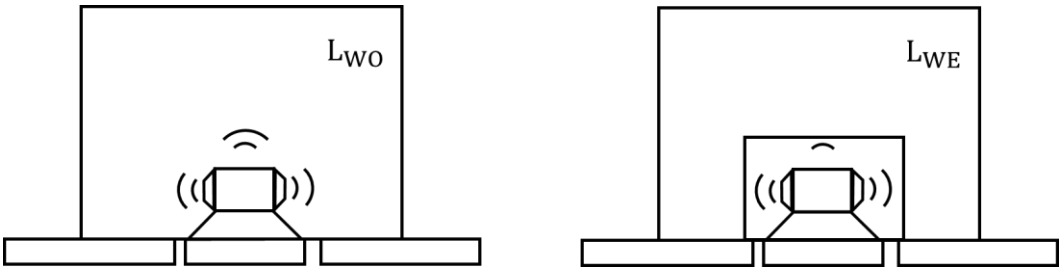

Figure 2.1 Definition of insertion loss [1].

2.2 Analytical Approaches to Determine Insertion Loss

There have been several prior analytical and numerical simulation models for enclosures. In one of the earliest studies, Jackson [2] created a crude approximation of an enclosure by modeling the source and enclosure as two separate infinite panels. The source panel was given a constant volume velocity while the receiver panel was assumed to be a limp panel. Plane wave propagation was assumed in the air space between the two panels and the calculated displacement amplitude ratio in decibels of the source and enclosure panels was defined as the insertion loss. Note that this model assumes that the enclosure is sealed and did not take into account the enclosure modes. Nonetheless, it is an adequate approximation for sealed enclosures at middle and high frequencies where sound transmission through the panel is dominant.

Junger [3] improved the model by simulating the source as a vibrating piston and the enclosure wall as a finite rectangular plate. Junger noted that there was a trough in the insertion loss at low frequencies which corresponded to the wall modes. Absorptive material was also incorporated in the theoretical model.

Tweed and Tree [4] performed measurement studies using an unlined and lined sealed enclosure, and compared to the aforementioned analytical models. It was concluded that both theoretical models failed to provide an adequate insertion loss prediction and pointed to the need for further work.

Hillarby [5] developed both a low and high frequency sealed enclosure model. The low frequency model utilizes a mode matching scheme. It is assumed

that a uniform acoustic pressure is distributed across the enclosure panels so that only modes in a single direction are considered. The model did not take the geometry of the source into account. At higher frequencies, a statistical energy analysis approach was used to predict the performance. Though a significant improvement to the previous work, the source and enclosure geometry was not captured realistically in the model, and the enclosure was assumed to be sealed.

Sharp [6] performed an extensive campaign to examine the effect of transmission loss through various common single and double panel wall constructions. Much of this work is directly applicable to sealed enclosures where the transmission path is through the enclosure wall.

More recently, Sgard et al. [7] developed a more realistic hybrid method for large enclosures which combined SEA and the method of image sources for the direct field. Two types of enclosures (parallelepipedic and L-shaped geometries) were built to investigate the feasibility of the hybrid approach. The models were validated by comparing to sound pressure level measurements inside the enclosure and to insertion loss measurements. Sgard et al. [7] looked at 26 configurations to more fully investigate the effect of important parameters such as enclosure geometry, panel materials, noise control treatments, location of the source inside the enclosure, and the presence of an opening. The results demonstrated that an image source model coupled with SEA was a reliable tool for enclosure evaluation. However, the model did not predict the lower frequency enclosure resonances.

Vér [1] in the well-known *Noise and Vibration Control Engineering: Principles and Applications* provides one of the most extensive practical guides on the design of enclosures. However, the text primarily deals with sealed enclosures and only briefly looks at partial enclosures though these are most commonly used to reduce rotating machinery noise. Vér's equation is simple and is based on the percentage of open area and sound absorptive coverage. The results are adequate for the most part at higher frequencies where sound absorption is the predominant mechanism for enclosure attenuation. Nevertheless, results do not take into account the low frequency enclosure air cavity modes that are of primary interest to designers.

2.3 Numerical Simulation Approaches to Determine Insertion Loss

Besides the analytical approaches reviewed, numerical simulation has been used to determine the insertion loss of partial enclosures. The boundary element method (BEM) has generally been the method used. For instance, Augusztinovicz et al. [8] used BEM to determine the insertion loss of engine enclosures where the source was modeled as a collection of point sources. Even though the results proved the feasibility of the approach and matched with measurement results qualitatively, there were still significant differences between simulation and measurement. Results were reported in 1/3-octave bands and low frequency enclosure acoustic modes were not included.

Similarly, Zhou et al. [9] validated a boundary element model to assess the performance of a steel partial enclosure with dimensions $0.48 \times 0.48 \times 0.66\ \mathrm{m}^3$.

The enclosure had one or two openings and sound absorptive material lined on one side panel. Results were compared with measurement with excellent agreement. Most importantly, low frequency acoustic resonances were successfully identified. A numerical sensitivity study was conducted to determine the effects of enclosure size, opening size, and sound absorptive coverage. Opening size proved the most important consideration.

2.4 Application of Resonators in Enclosures

The primary approach to improve the low frequency performance of partial enclosures is to add resonators. Several researchers have investigated adding resonators to sealed enclosures. For instance, Fahy and Schofield [10] used an analytical modal approach to examine the placement of a single Helmholtz resonator into a small rectangular airspace ($\mathrm{V} = 13.3\ m^3$). The resonator had a volume range from 0 to 8×10^{-3} m^3, a neck length of 150 mm, and a neck diameter 102 mm. Measured and analytical results compared well and with a demonstrable improvement in the sealed enclosure performance. Cummings [11] developed a multi-mode model to determine the attenuation if a resonator array is inserted in a sealed enclosure. Over 10 dB reductions of the interior sound pressure were noted at the resonance frequencies.

Estève and Johnson [12] applied Helmholtz resonators to reduce the sound transmission within a sealed cylindrical shell. Helmholtz resonators were used in conjunction with distributed vibration absorbers (DVA). Results demonstrated

that the Helmholtz resonator could reduce the interior noise by 3.8 dB while the DVA and Helmholtz resonator combination reduced the noise by 7.7 dB in the 50-160 Hz band. The study also illustrated that the noise reduction resulting from the treatment decreased as the system damping ratio increased.

In similar work, Yu and Cheng [13] utilized a T-shaped acoustic resonator which could be located at a single position but still provide multiple acoustic resonances. The location of the T-shaped resonator was optimized for a small enclosure with dimensions $0.98 \times 0.70 \times 1.19$ m^3. There was acceptable agreement between simulation and experiments.

2.5 Fundamental Acoustic Background for Plane Wave Approach

The fundamental theory that will be used for the theoretical development in Chapter 3 is surveyed in the remainder of the chapter.

2.5.1 Transfer Matrix Theory

The transfer matrix [14] is a convenient tool for one-dimensional analysis in acoustics. Sound pressure and particle velocity at the left and right ends of an acoustic element can be related using a four-pole transfer matrix. The transfer matrix for a straight duct (Figure 2.2) can be written as

$$\begin{Bmatrix} p_1 \\ u_1 \end{Bmatrix} = \begin{bmatrix} \cos(kl) & i\rho c \sin(kL) \\ \frac{i}{\rho c}\sin(kl) & \cos(kL) \end{bmatrix} \begin{Bmatrix} p_2 \\ u_2 \end{Bmatrix} \tag{2-2}$$

where k is the complex wavenumber defined as ω/c and l is the length of the duct element. ω and c are the angular frequency in rad/s and speed of sound respectively.

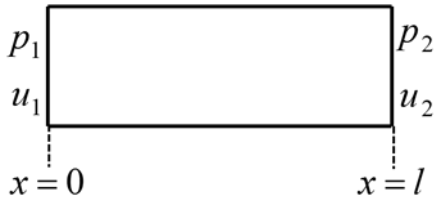

Figure 2.2 Definition of transfer matrix.

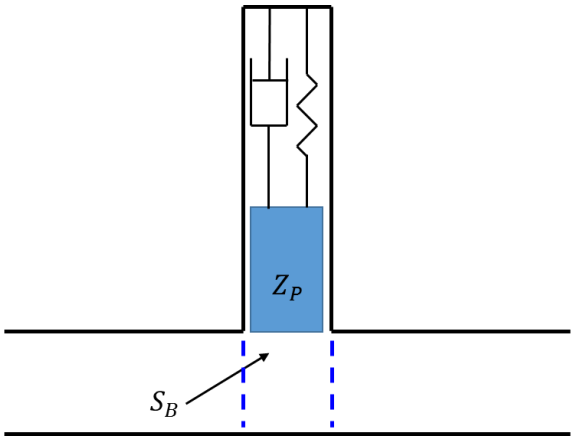

Figure 2.3 Schematic of side branch.

Resonators are generally modeled as a parallel or branch impedance as illustrated in Figure 2.3. In that case, it is assumed that the sound pressure across the parallel element is constant and the transfer matrix is expressed as

$$\begin{Bmatrix} p_1 \\ u_1 \end{Bmatrix} = \begin{bmatrix} 1 & 0 \\ 1/Z_p & 1 \end{bmatrix} \begin{Bmatrix} p_2 \\ u_2 \end{Bmatrix} \tag{2-3}$$

where Z_p is the parallel or branch impedance.

2.5.2 Resonator Theory

Resonators function by placing a low impedance at a frequency of interest at the side branch insertion point. This is equivalent to an electrical short circuit. The wave propagating down the main duct is attenuated via interference at the resonator insertion region The most commonly used resonators are quarter wave and Helmholtz resonators. Resonators are effective at the frequencies they are designed for and may produce unwanted resonances in the sidebands. Though resonators are place inside of a partial enclosure in this research, the attenuation mechanism is the same as that for mufflers.

A quarter wave resonator is a simple side branch which is made up of a duct with a constant cross-sectional area and hard termination as shown in Figure 2.4. The particle velocity at the end of the duct is assumed to be zero. It follows that the impedance of the quarter wave resonator at the junction may be expressed as

$$Z_{\boldsymbol{B}} = -\frac{i\rho c}{S_B}\cot(kL) \tag{2-4}$$

where L is the length of the duct and S_B is the cross-sectional area of the branch. The maximum noise attenuation occurs if $Z_{\boldsymbol{B}} = 0$. This will be the case when

$$kL = \frac{n\pi}{2}, n = 1,3,5, \ldots \tag{2-5}$$

$$f_n = \frac{nc}{4L}, n = 1,3,5, \ldots \tag{2-6}$$

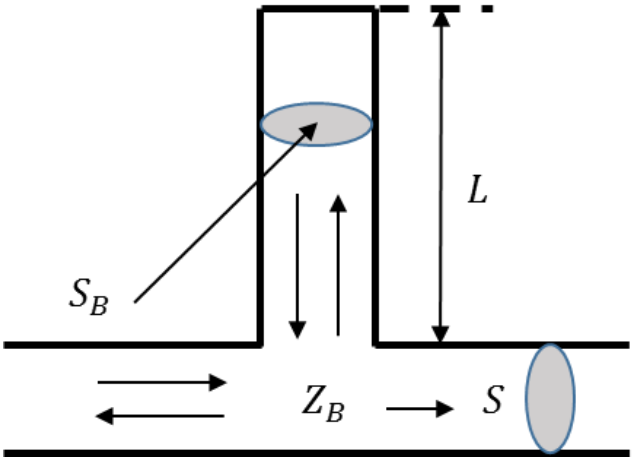

Figure 2.4 Schematic of quarter wave resonator.

Helmholtz resonators are also commonly used. They are analogous to a mechanical mass and spring and may be thought of as a tuned dynamic absorber consisting of a short duct or neck (mass) attached to a larger air cavity (air spring) as shown in Figure 2.5. The inlet impedance of the Helmholtz resonator is expressed as

$$Z_{\boldsymbol{B}} = i\omega\rho L + \rho c^2 S_B / i\omega V \tag{2-7}$$

where V is the volume of the cavity, L is the neck length, and S_B is the cross-sectional area of the neck. The maximum noise attenuation is obtained if $Z_B = 0$ which corresponds to a frequency of

$$f_r = \frac{c}{2\pi}\sqrt{\frac{S_B}{LV}} \tag{2-8}$$

Usually, it is necessary to adjust the neck length L by adding an end correction to account for some additional mass of air on either side of the neck. This equivalent neck length can be expressed as

$$L_{eq} = L + \Delta L \tag{2-9}$$

in which, ΔL is the end correction and can be approximately expressed as

$$\Delta L = 0.82 d_B / 2 \tag{2-10}$$

where d_B is the diameter of the side branch.

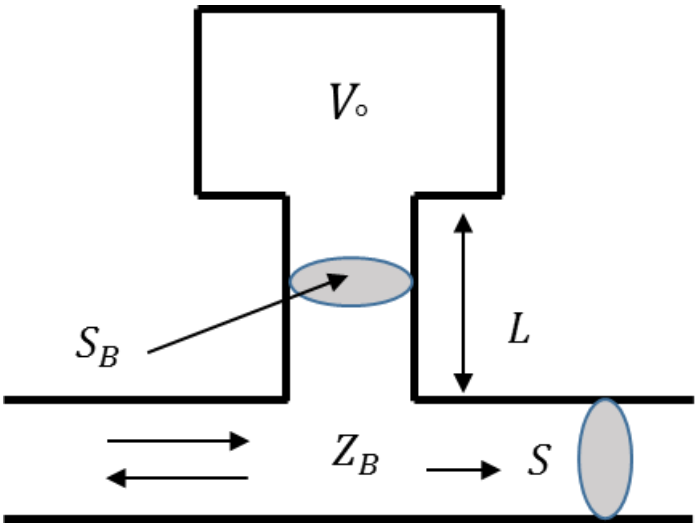

Figure 2 5 Schematic of Helmholtz resonator.

2.5.3 Opening Impedance

The impedance at an aperture can be approximated as that for the end of a flanged or unflanged duct termination. Figure 2.6 shows the flanged and unflanged cases. It is recognized that this is an approximation since the duct length is approximately the thickness of the enclosure itself.

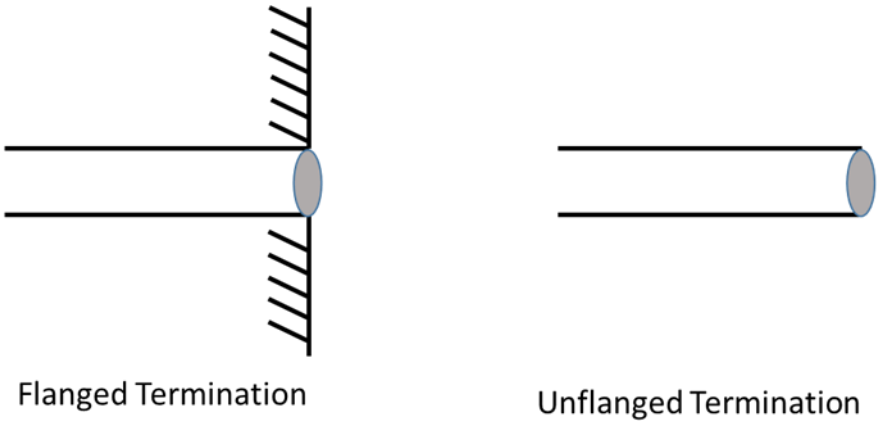

Figure 2.6 Schematic of flanged termination and unflanged termination.

The termination impedance (Z_{rad}) [15] for the flanged case is expressed as

$$Z_{rad} = \frac{\rho c}{S}(R_1(2ka) - jX_1(2ka)) \tag{2-11}$$

where

$$R_1 = 1 - \frac{J_1(2ka)}{ka} \quad X_1 = \frac{H_1(2ka)}{ka} \tag{2-12}$$

and J_1 and H_1 are the first order Bessel function and Struve function, respectively.

For an unflanged termination [16], the radiation impedance (Z_{rad}) is defined as

$$Z_{rad} = \frac{\rho c(1+R)}{S(1-R)} \tag{2-13}$$

where the reflection coefficient (R) is expressed as

$$R = -R_0 e^{-j2ka\zeta_0} \tag{2-14}$$

and a is the radius at the opening, R_0 is the amplitude of the reflection coefficient and ζ_0 is an end correction term. The amplitude of the reflection coefficient (R_0) is defined as

$$R_0 = 1 + 0.01226ka - 0.059079(ka)^2 + 0.033576(ka)^3 - 0.06432(ka)^4, \quad ka < 1.5 \tag{2-15}$$

and the end correction ζ_0 is written as

$$\zeta_0 = \begin{cases} 0.6133 - 0.1168(ka)^2, & ka < 0.5 \\ 0.6393 - 0.1104ka, & 0.5 < ka < 2 \end{cases} \tag{2-16}$$

2.5.4 Acoustic Source Modeling

A point monopole source is a simple, theoretical representation of an acoustic source. It is convenient to utilize since it has negligible geometry. The sound pressure radiated from a point source is

$$p(r) = A\frac{e^{-ikr}}{r} \tag{2-17}$$

where k is the wave number, and r is the distance between the measured field point and the source. The sound power radiated from the point source does not depend on the distance and can be written as

$$W_i = \frac{1}{4\pi}\rho c k^2 Q^2 \tag{2-18}$$

where Q is the volume velocity of the point source.

CHAPTER 3 ENCLOSURE MEASUREMENT AND SIMULATION

3.1 Introduction

Acoustic enclosures are widely used in industry to reduce machinery noise. There are two primary noise propagation paths: structureborne and airborne. The structureborne path is from the rotating machinery, through the mounting, and into the enclosure which radiates sound. If machinery is properly isolated, the structureborne path can normally be controlled though flanking paths are often troublesome. The other path is airborne propagation from the machinery into the enclosure space, and through the openings. The airborne path can be controlled at high frequencies by affixing sound absorption to the inside enclosure walls and avoiding a direct line of sight path from the source to a receiver. However, enclosure acoustic resonances are unavoidable at low frequencies where sound absorption is ineffective. If the rotating speed of the enclosed machinery corresponds with a low frequency resonance, a noise problem is probable.

Enclosure walls act as a barrier, and are usually fabricated from heavy plastic or steel to reflect the sound. There is some space between the enclosure and enclosed machine, and vibration isolators are placed in between the machine and enclosure base to minimize structureborne energy propagation into the enclosure walls which have large surface area. Most enclosures have openings to meet requirements for ventilation or to act as passageways for wires and pipes

coming and going. These openings become the primary noise path especially at frequencies matching the first few acoustic resonances.

In this work, plane wave approaches are used to determine the insertion loss of partial enclosures at low frequencies. The suggested model is amenable to geometrically complex enclosures and sources. Most importantly, the model can be used to identify the first few acoustic resonances which manifest themselves as troughs in the insertion loss. These frequencies, in which the enclosure amplifies the acoustic source, are unavoidable, and it should be insured that the prime mover does not operate at these frequencies for extended periods of time.

3.2 Experiment setup

All experiments were performed in the hemi-anechoic chamber at the University of Kentucky. Insertion loss was measured and determined via sound intensity scanning. First, a bookshelf speaker was located at the center of the chamber, and a frame was built up to create 5 scanning surfaces for intensity scanning. It is shown in the Figure 3.1. An enclosure was constructed from 1.9 cm thick particle board, shown in Figure 3.2. The source was then enclosed and the sound power measured again. Figure 3.3 shows how the speaker was installed in the enclosure. Insertion loss was calculated as the difference between the two sound power measurements in dB. Subsequent measurements for parameter study, validation cases and modification cases were carried out using the same method.

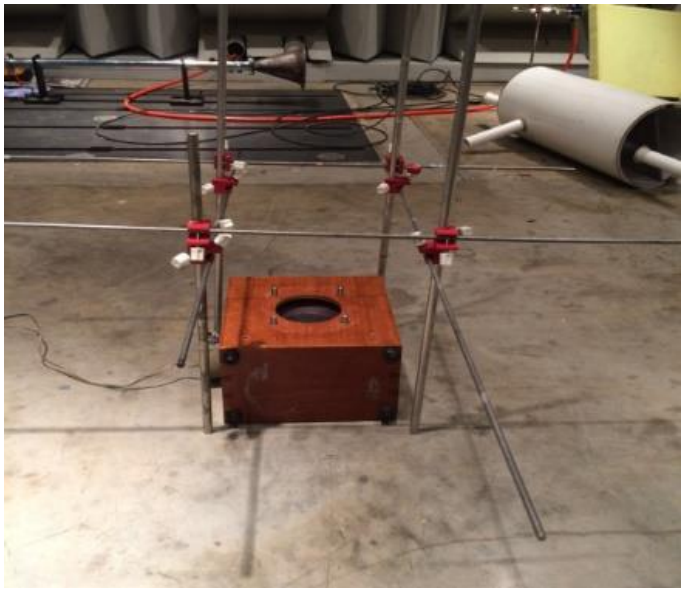

Figure 3.1 Bookshelf loud speaker on floor.

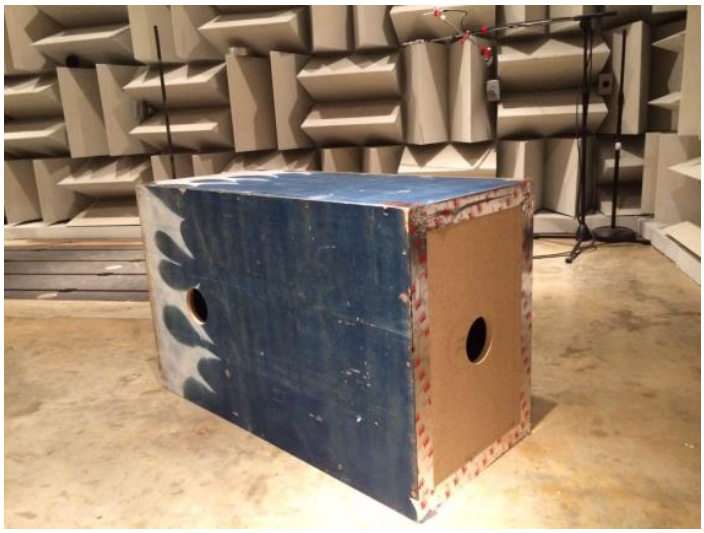

Figure 3.2 Photograph of partial enclosure.

Figure 3.3 Photograph of loudspeaker inside of partial enclosure.

3.3 Acoustic Finite Element Analysis Strategy

The acoustic finite element method (FEM) was used to simulate each case. Figure 3.4 shows a schematic of the modeling procedure. Acoustic finite elements are used to model the airspace inside the enclosure and adjacent to the enclosure on the outside. Boundaries are modeled using a reflection free boundary condition which has been termed a perfectly matched layer in the literature [17, 18, 19, 20]. The approach insures a reflection free boundary for waves having varying angles of incidence. The particular implementation in Siemens Virtual. Lab is referred to as an automatically matched layer (AML) boundary condition [21] because the software internally creates the PML mesh and then adjusts the mesh thickness and resolution at each frequency. AML boundaries are indicated in Figure 3.5.

The acoustic mesh consists entirely of linear tetrahedral elements and the structural mesh of linear quadrilateral shells. The mesh was created using ANSYS APDL [22]and then solved using Siemens Virtual. Lab. The solution is fully coupled. A bookshelf loudspeaker is assumed to be the source and the external geometry of the loudspeaker is modeled. A unit velocity is assumed on the speaker diaphragm.

Insertion loss is determined by direct application of Equation (2-1). Models are created for both the source and the source plus enclosure, and the difference in sound power in dB is subtracted. For the enclosed model, AML surfaces are used to assess the sound power emitted through the openings and also from the structure. The airborne and structureborne emissions can be differentiated and compared if desired, but it was observed that the structureborne path was negligible compared to the airborne path.

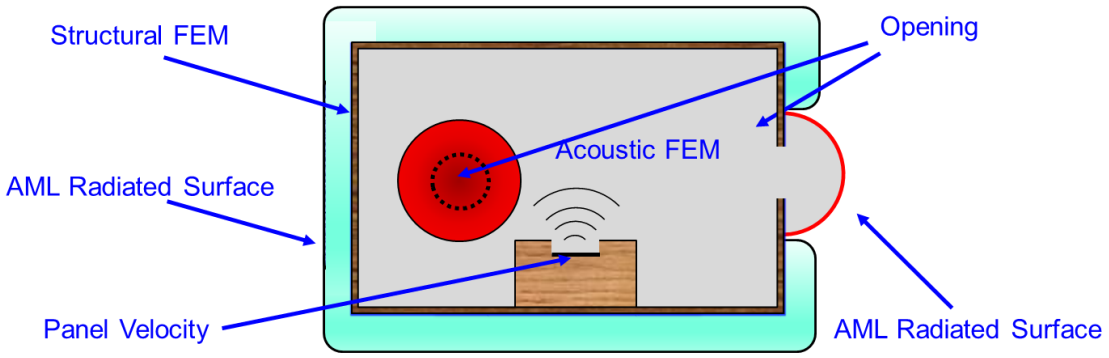

Figure 3.4 Schematic illustrating finite element simulation strategy.

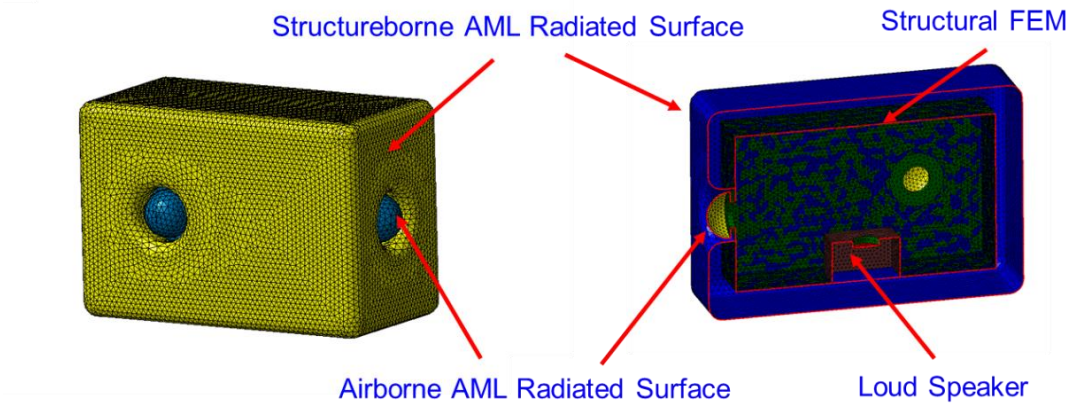

Figure 3.5 Acoustic finite element mesh showing AML surfaces.

3.4 Plane Wave Approach Methodology

The primary objectives of the analysis are to identify low frequency insertion loss troughs and to use the model to develop treatments. At high frequencies, the model will have limited use because sound absorption is effective and troughs in the insertion loss are less noticeable. All calculation was carried out using the numerical computing software MATLAB. The following assumptions are made.

1. Plane wave propagation is assumed for each direction independently.
2. Acoustic modes are well spaced in frequency.
3. Temperature is constant across each plane wave element.
4. Flow is ignored.

The Figure 3.6 shows a schematic of a volumetric source that is located in the enclosure. Assume plane wave propagation in one of the enclosure directions.

The volume velocity will be the sum of the volume velocities on each side of the source. Hence,

$$Q = S_L u_L + S_R u_R \tag{3-19}$$

where u_L, u_R and S_L, S_R are the respective particle velocities and cross-sectional areas to the right and left of the point source. The impedances (Z_L and Z_R) to the left and right of the point source can be written as

$$Z_L = \frac{p_L}{S_L u_L} \tag{3-20}$$

and

$$Z_R = \frac{p_R}{S_R u_R} \tag{3-21}$$

respectively. The equivalent impedance ((Z_{eq}) can be expressed as

$$Z_{eq} = \frac{p}{Q} = \frac{Z_L Z_R}{Z_L + Z_R} \tag{3-22}$$

Since $p = p_L = p_R$.

The impedances (Z_L and Z_R) on either side of the source can be determined using plane wave methods. A brief summary of the method is detailed below. Munjal's [14] classic text *Acoustics of Ducts and Mufflers* is recommended for more details.

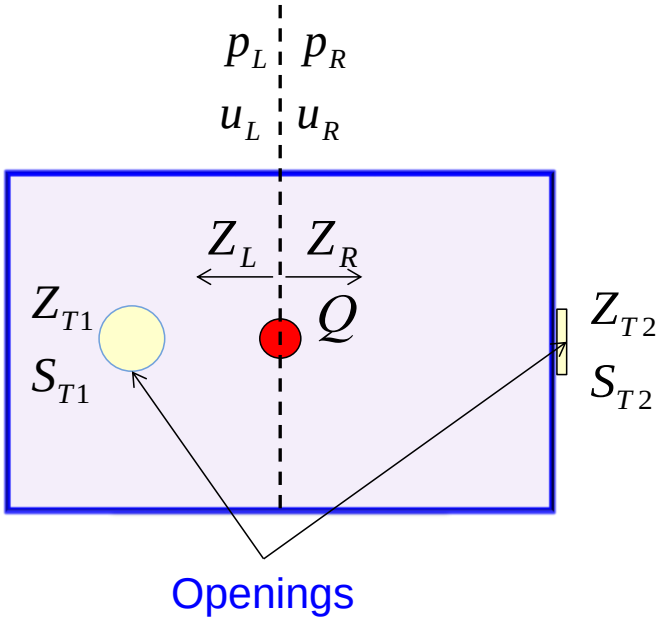

Figure 3.6 Schematic of enclosure showing variables.

The enclosure on either side of the source can be modeled as a cascade of ducts, and side branches terminating in an opening. The sound pressure and particle velocity on each side of a plane wave element can be expressed as

$$\begin{Bmatrix} p_1 \\ S_1 u_1 \end{Bmatrix} = \begin{bmatrix} T_{11} & T_{12} \\ T_{21} & T_{22} \end{bmatrix} \begin{Bmatrix} p_2 \\ S_2 u_2 \end{Bmatrix} \tag{3-23}$$

where T_{11}, T_{12}, T_{21}, and T_{22} are the transfer matrix elements. This convention is illustrated in Figure 3.7.

For a straight duct, the transfer matrix can be expressed as

$$\begin{Bmatrix} p_1 \\ S_1 u_1 \end{Bmatrix} = \begin{bmatrix} \cos(kL) & \left(\frac{j\rho c}{S_2}\right)\sin(kL) \\ \left(\frac{jS_1}{\rho c}\right) sin(kl) & \frac{S_1}{S_2}\cos(kL) \end{bmatrix} \begin{Bmatrix} p_2 \\ S_2 u_2 \end{Bmatrix} \quad (3\text{-}24)$$

where k is the wavenumber, l is the length, ρ is the mass density, and c is the speed of sound. For a side branch, the transfer matrix can be expressed as

$$\begin{Bmatrix} p_1 \\ S_1 u_1 \end{Bmatrix} = \begin{bmatrix} 1 & 0 \\ 1/Z_B & 1 \end{bmatrix} \begin{Bmatrix} p_2 \\ S_2 u_2 \end{Bmatrix} \quad (3\text{-}25)$$

where Z_B is the impedance of the side branch. The most common side branch impedance for enclosures is a quarter wave tube. The impedance of which can be expressed as

$$Z_B = -j\frac{\rho c}{S_B}\cot(kl_B) \quad (3\text{-}26)$$

where l_B and S_B are the length and area of the side branch respectively.

The impedance at the opening (Z_T) is approximated as that for a baffled termination [15]. Hence,

$$Z_T = \frac{\rho c}{S_a}(R_1 - jX_1) \quad (3\text{-}27)$$

where

$$R_1 = 1 - \frac{J_1(2ka)}{ka} \tag{3-28}$$

and

$$X_1 = \frac{H_1(2ka)}{ka} \tag{3-29}$$

with J_1 and H_1 corresponding to the Bessel and Struve functions of the first order respectively.

The transfer matrices for the individual elements can be multiplied together in order to identify the transfer matrix ($[A]$) from the source to the termination. Accordingly,

$$\begin{bmatrix} A_{11} & A_{12} \\ A_{21} & A_{22} \end{bmatrix} = [T_1][T_2][T_3] \dots [T_N] \tag{3-30}$$

where $[T_i]$ are the individual transfer matrices for the different duct elements assuming there are N duct elements. The impedance on either side of the source (Z_m with $m = L$ or R) can be written as

$$Z_m = \frac{A_{11}^{(m)} Z_T^{(m)} + A_{21}^{(m)}}{A_{21}^{(m)} Z_T^{(m)} + A_{22}^{(m)}} \tag{3-31}$$

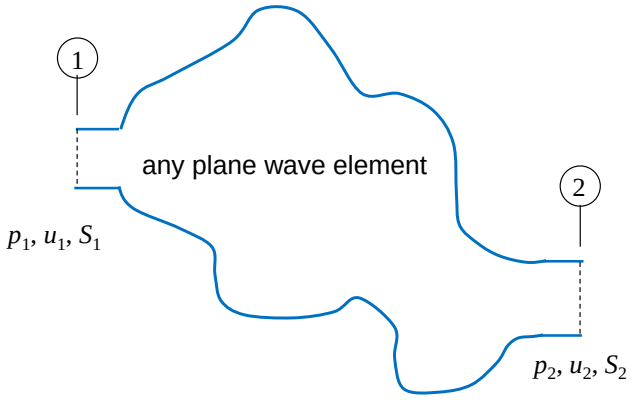

Figure 3. 7 Schematic showing a plane wave element.

The insertion loss for the partial enclosure with openings is determined as follows. First, assume a unit volume velocity (Q) for the source. The sound power from the unenclosed source (W_{wo}) is expressed as

$$W_{wo} = \frac{1}{4\pi}\rho c k^2 Q^2 \tag{3-32}$$

The sound power for the enclosed source is found by first determining the impedance to the left and right of the source (Z_L and Z_R) using plane wave theory. Then, determine the equivalent impedance (Z_{eq}) and sound pressure at the source (p) using Equation (3.30). The particle velocities on each side of the source (u_L and u_R) can be found via Equations (3.28) and (3.29). Using the transfer matrix from the source to the opening, the sound pressure (p_k) and particle velocity (u_k) for opening k can be determined on either side of the source using

$$\begin{Bmatrix} p_k \\ S_k u_k \end{Bmatrix} = \begin{bmatrix} B_{11}^{(k)} & B_{12}^{(k)} \\ B_{21}^{(k)} & B_{22}^{(k)} \end{bmatrix}^{-1} \begin{Bmatrix} p_m \\ S_m u_m \end{Bmatrix} \tag{3-33}$$

where p_m and u_m are the respective sound pressure and particle velocity on the appropriate side of the source where $m = L$ or R. The sound power from the enclosed source can then be expressed as

$$W_{enc} = \sum_{k=1}^{N} \frac{1}{2} \mathrm{Re}(p_k u_k^*) S_k \tag{3-34}$$

where k is an index for the opening and N is the number of openings. p_k, u_k, and S_k are the respective sound pressure, particle velocity, and cross-sectional area at the opening. The insertion loss due to the enclosure (IL) can be expressed as

$$IL = L_{W_{wo}} - L_{W_{enc}} \tag{3-35}$$

where $L_{W_{wo}}$ and $L_{W_{enc}}$ are the sound powers of the source and enclosed source in dB.

The procedure can be carried out in all three coordinate directions. After doing so, the insertion loss is determined for all three directions individually and the lowest insertion loss is selected. This assumes that troughs in the insertion loss are primarily due to resonances and that these resonances are well separated from one another.

3.5 Baseline Case Results

The procedure was tested using the enclosure setup shown in Figure 3.8. A $96 \times 58 \times 41$ cm^3 enclosure was constructed from 1.9 cm thick particle board. A bookshelf loudspeaker was positioned at the center of the enclosure in the floor. There are two 10 cm diameter circular openings: one located on one end of the enclosure and the other on the front side as shown in Figure 3.8. A photograph of the box with loudspeaker inside is shown in Figure 3.9.

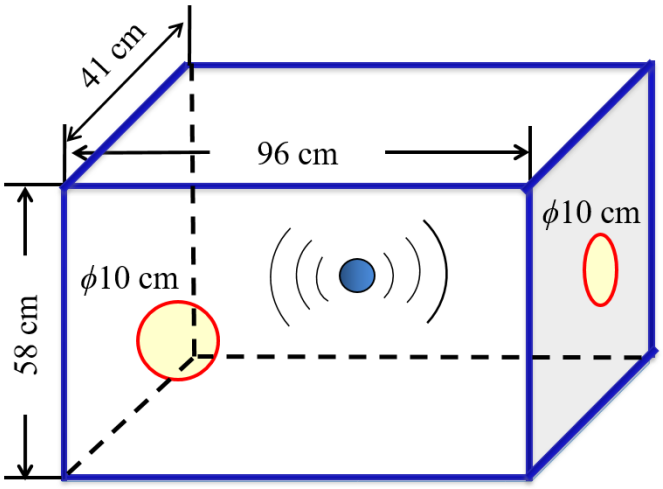

Figure 3.8 Schematic showing baseline enclosure and important dimensions.

Figure 3.9 Schematic showing baseline enclosure with loudspeaker placement.

Schematics showing plane wave models in both the lengthwise, vertical, and lateral directions are shown in Figures 3.10, 3.11, and 3.12 respectively. The figures indicate how the enclosure airspace was subdivided into plane wave elements and Tables 3.1, 3.2, and 3.3 indicate the respective dimensions for the plane wave elements. In the approach used, the opening was considered as the termination in each case though this is not essential to using the method. More information regarding breaking complex geometry up into plane wave elements is available in Reference [23].

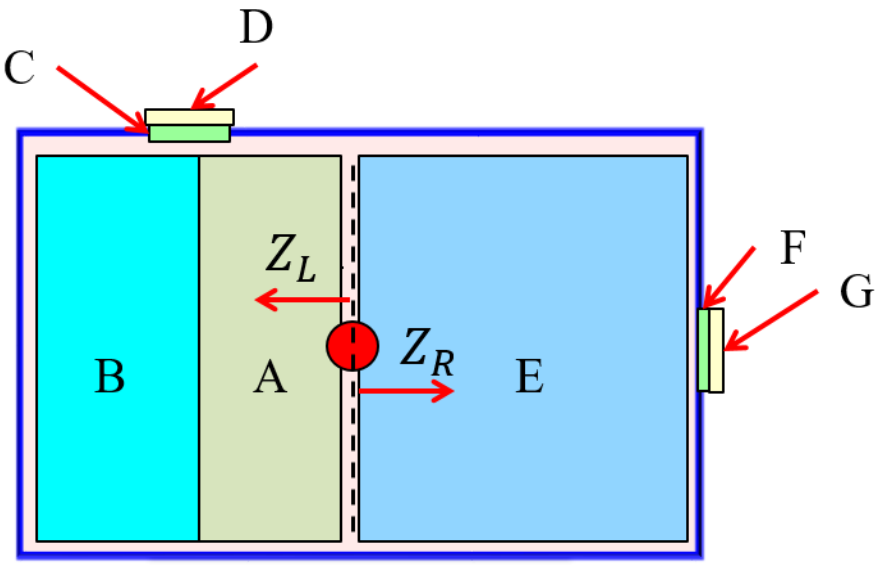

Figure 3.10 Schematic showing plane wave strategy in the lengthwise direction for baseline enclosure.

Table 3.1 Plane Wave model dimensions in longitudinal direction for baseline enclosure.

Element	Type	Length (cm)	Area (cm^2)
A	Duct	24	2690
B	Quarter Wave Tube	24	2690
C	Duct	1	79
D	Termination Impedance	N/A	79
E	Duct	48	2690
F	Duct	1	79
G	Termination Impedance	N/A	79

.

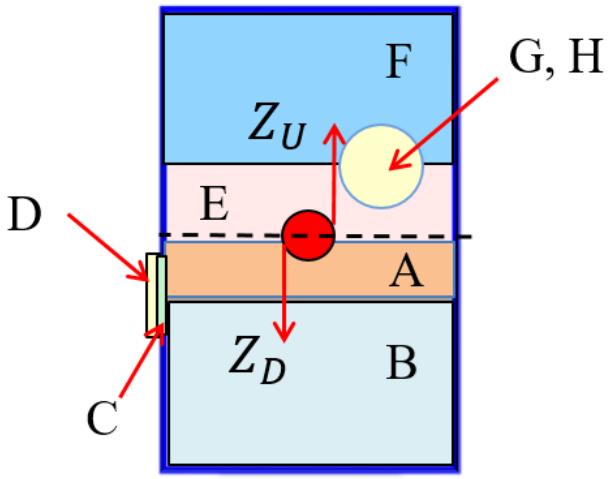

Figure 3.11 Schematic showing plane wave strategy in the vertical direction for baseline enclosure.

Table 3.2 Plane wave model dimensions in vertical direction for baseline enclosure.

Element	Type	Length (cm)	Area (cm^2)
A	Duct	10	3940
B	Quarter Wave Tube	19	3940
C	Duct	1	79
D	Termination Impedance	N/A	79
E	Duct	10	3940
F	Quarter Wave Tube	19	3940
G	Duct	1	79
H	Termination Impedance	N/A	79

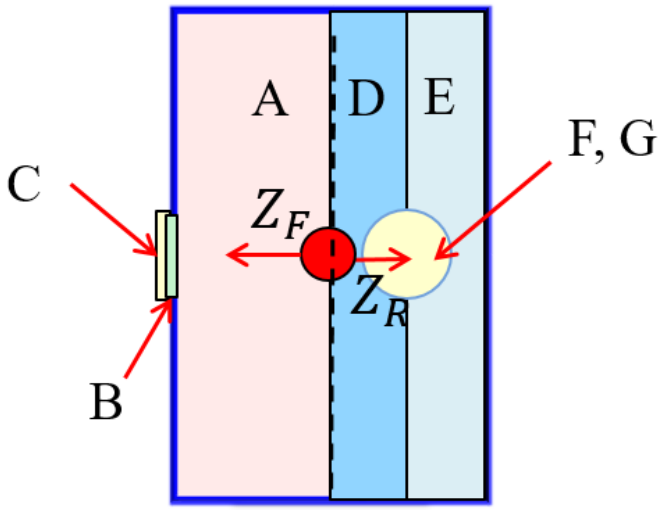

Figure 3.12 Schematic showing plane wave strategy in the lateral direction for baseline enclosure.

Table 3.3 Plane wave model dimensions in longitudinal direction for baseline enclosure.

Element	Type	Length (cm)	Area (cm^2)
A	Duct	21	5610
B	Duct	1	79
C	Termination Impedance	N/A	79
D	Duct	10	5610
E	Quarter Wave Tube	10	5610
F	Duct	1	79
G	Termination Impedance	N/A	79

Figure 3.13 compares the insertion loss from plane wave simulation to the sound power determined using measurement and FEM simulation. It can be seen that the plane wave method compares reasonably well with FEM simulation. Though plane wave simulation over predicts the peaks and troughs of insertion loss, it correctly identifies the enclosure resonances which are most important for design purposes. There is some discrepancy below 30 Hz in both plane wave and FEM simulation. However, results are generally not so important at frequencies that are so low.

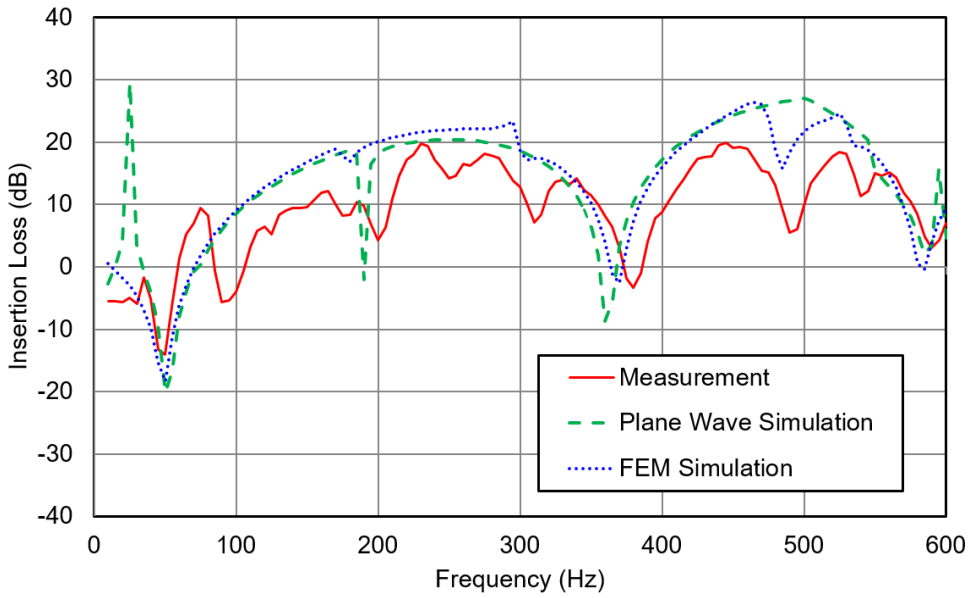

Figure 3.13 Insertion loss comparison for bassline case showing measurement, plane wave simulation and finite element simulation.

3.6 Validation Case-Large Source

The feasibility of the approach for larger sources was then examined. For this example, results from plane wave simulation were compared to acoustic FEM simulation alone and not to measurement. The source geometry was modeled as a box as shown in Figure 3.14. The dimensions of the source box are $50 \times 50 \times 35$ cm^3. In order to generate the boundary conditions for the *box source* in the acoustic FEM model, a point source was centered in an imaginary box of the same size and the particle velocities of the radiated field were calculated on the surface of the imaginary box. Those determined particle velocities were then used as boundary conditions on the surface of the source box. Thus, the *box source* will produce an identical sound field to a point source if it is located in a free space. The sound power from the box source is assumed to be unity and the sound power of the enclosed *box source* was determined using FEM analysis in order to identify the insertion loss.

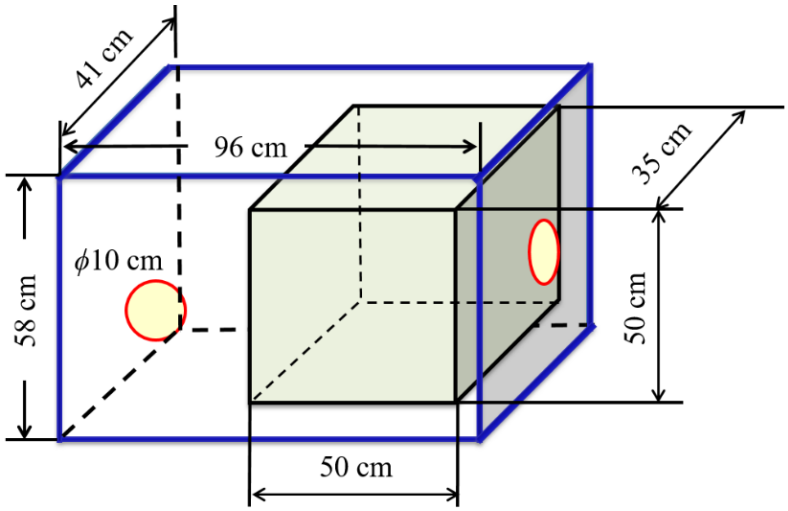

Figure 3.14 Schematic showing enclosure with box shaped source.

Figure 3.15 shows a schematic of the plane wave model that was created to simulate the longitudinal direction. Similar plane wave models were developed for the other two directions as well. Table 3.4 shows the dimensions used for the individual duct elements in the longitudinal direction. Notice that region of the enclosure that the source box occupies is treated as a duct having cross-sectional area equivalent to that of the airspace surrounding the box source.

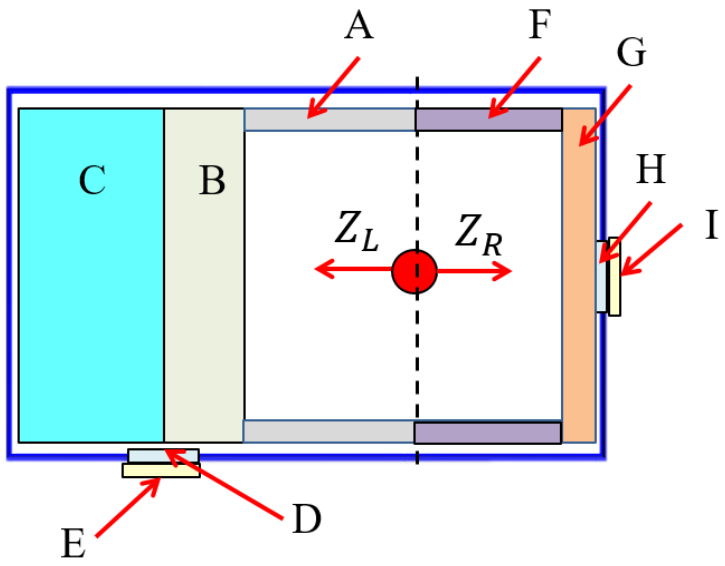

Figure 3.15 Schematic showing plane wave strategy for enclosure with box shaped source.

Figure 3.16 compares the insertion loss determined by the plane wave and BEM methods. There is good agreement up to approximately 350 Hz which should be sufficient for many engine enclosure applications. More importantly, the insertion loss troughs of primary interest to designers at 65, 155, and close to 320 Hz are successfully identified. This example demonstrates that the procedure suggested may be applied to enclosures having a large source located within.

Table 3.4 Plane wave model dimensions in longitudinal direction for enclosure with box shaped source.

Element	Type	Length (cm)	Area (cm^2)
A	Duct	24	94
B	Duct	14	2690
C	Quarter Wave Tube	24	2690
D	Duct	1	79
E	Termination Impedance	N/A	79
F	Duct	26	94
G	Duct	8	2690
H	Duct	1	79
I	Termination Impedance	N/A	79

Figure 3.16 Insertion loss comparison for enclosure with box shaped source

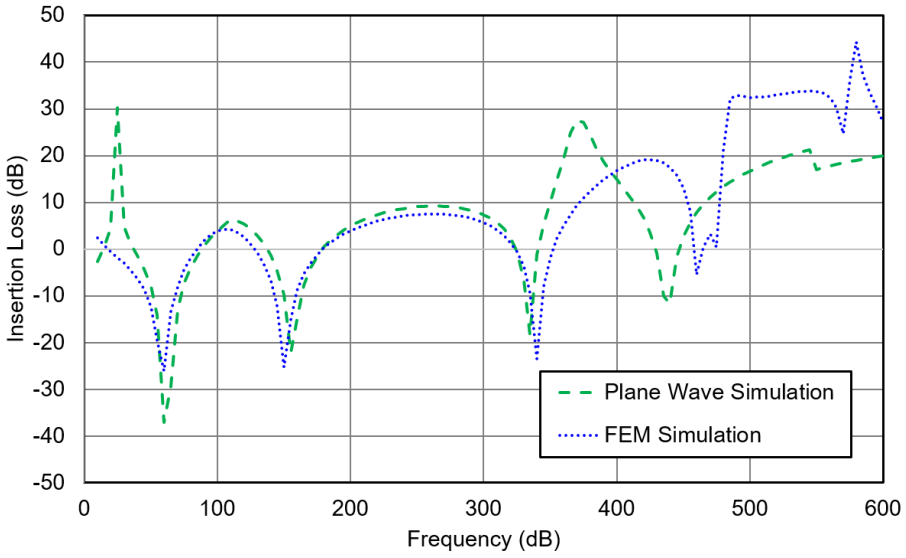

showing plane wave simulation, and finite element simulation.

.

3.7 Summary

A plane wave simulation approach for determining the low frequency insertion loss has been developed and has been validated via both BEM simulation and measurement. It has been shown that the approach can be successfully used to determine the troughs corresponding to acoustic resonances in the insertion loss. If the source has a fundamental or harmonics at one of these frequencies, the partial enclosure may amplify the sound and will not perform as well as expected.

The approach detailed has a number of advantages. After a model is developed, the effect of geometric changes can be assessed rapidly. Additionally, the method introduces intuition into the design process so that resonators can be considered and properly positioned in the enclosure. Though plane wave simulation may over predict the amount of improvement, strategies can nonetheless be evaluated and compared to one another. After plane wave simulation is used to determine a possible design, the design can be evaluated using a model having greater fidelity. For example, acoustic FEM or BEM might be used. At the present time, the primary failing of the method is that it does not include structural effects which may be important at lower frequencies.

CHAPTER 4 MODIFICATION CASES

One of the most effective means of dealing with acoustic resonances is to insert a resonator into the enclosure. Resonators shift the frequencies of the acoustic resonances, but will not eliminate resonances altogether. Nonetheless, operating frequencies of prime movers can be avoided. Moreover, the insertion loss at the operating frequencies can be increased.

In this chapter, three modification cases were investigated to improve the performance of the enclosure at low frequency domain. Two quarter wave resonators and one Helmholtz resonator were placed in sequence inside the enclosure to eliminate resonance issues at 365 Hz.

4.1 Quarter Wave Resonators

The enclosure used in Test Case 1 was then fitted with a quarter wave tube on one end. Several configurations were considered. The first is shown in Figure 4.1. The quarter wave tube is constructed as a U-shaped channel that follows the inner perimeter of the enclosure. The cross-sectional area of the channel is 23.5 cm^2 and the channel has a depth of 24 cm. The opening of the quarter wave tube is close to the end of the box. The plane wave model is shown for the lengthwise direction in Figure 4.2. Table 4.1 indicates the dimensions of the plane wave elements. Insertion loss results are shown in Figure 4.3. It can be seen that plane wave simulation correctly predicts that the insertion loss will increase considerably at 375 Hz. Measurement indicates an improvement of approximately 20 dB which

is also predicted by the FEM simulation. Though plane wave simulation over predicts the improvement, it does correctly identify the frequency of expected improvement.

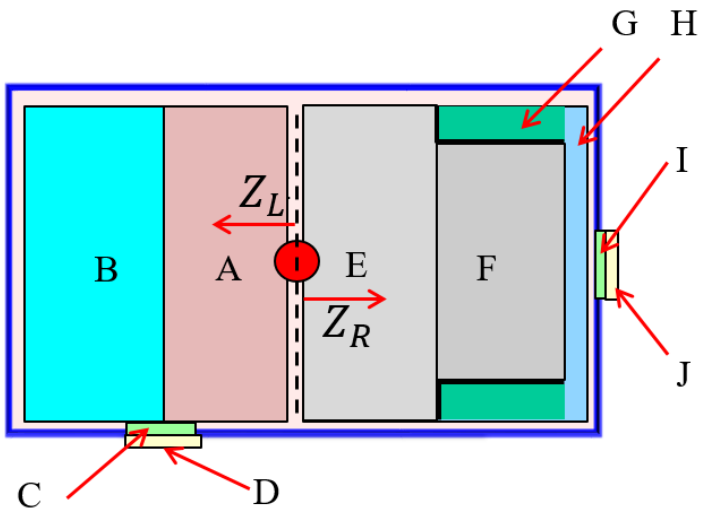

Figure 4.1 Schematic showing partial enclosure with quarter wave tube (opening on right side of channel).

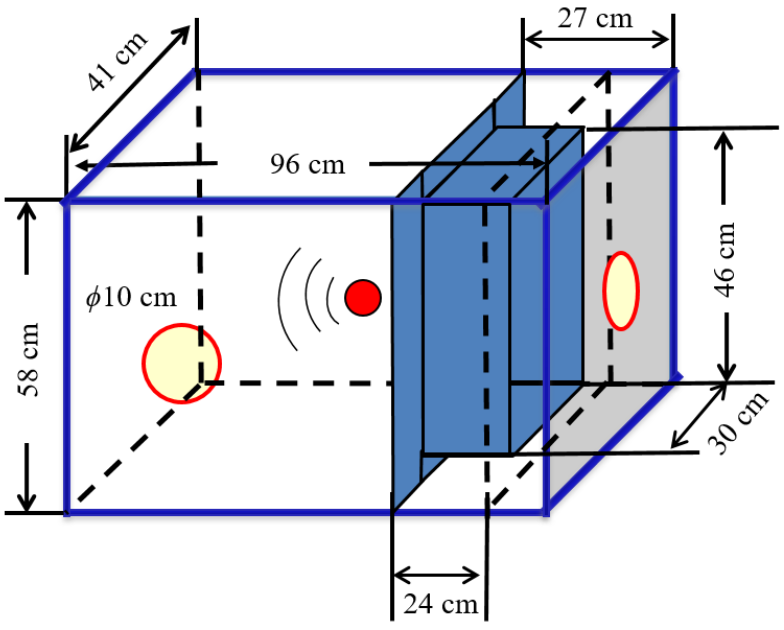

Figure 4.2 Schematic showing plane wave strategy for partial enclosure with quarter wave tube (opening on right side of channel).

Table 4.1 Plane wave model dimensions in longitudinal direction for test case-large quarter wave tube (opening on right side of channel).

Element	Type	Length (cm)	Area (cm^2)
A	Duct	24	2690
B	Quarter Wave Tube	24	2690
C	Duct	1	79
D	Termination Impedance	N/A	79
E	Duct	21.5	2690
F	Duct	23.5	1684
G	Quarter Wave Tube	23.5	1006
H	Duct	3	2690
I	Duct	1	79
J	Termination Impedance	N/A	79

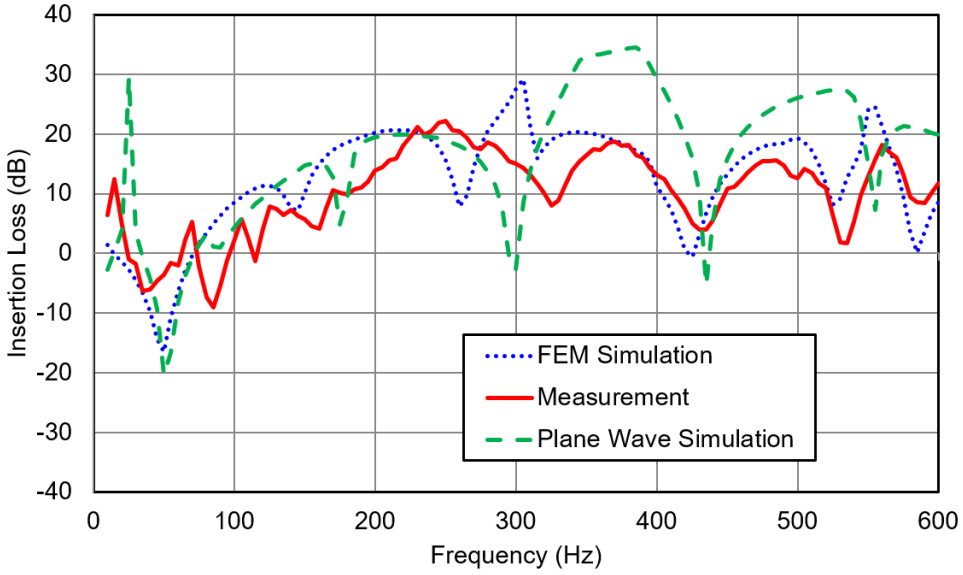

Figure 4.3 Insertion loss comparison for enclosure with quarter wave tube (opening on right side of channel) showing measurement, plane wave, and finite element simulation.

In the second configuration shown in Figure 4.2, the opening is positioned 16 cm from the end of the enclosure. The plane wave model in the lengthwise direction is shown in Figure 4.5. Table 6 provides the important dimensions for the plane wave model. Insertion loss results are shown in Figure 4.6. It can be seen that the insertion loss does not improve significantly at 375 Hz. The results demonstrate that the quarter wave tube does not substantially improve the enclosure performance if it the opening is placed close to the node line of the acoustic mode where the sound pressure is low.

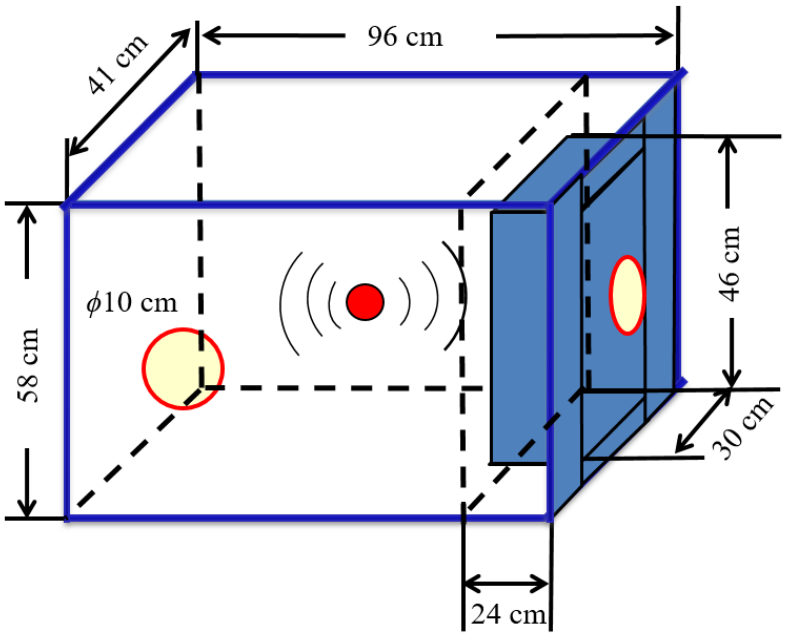

Figure 4.4 Schematic showing partial enclosure with quarter wave tube (opening on left side of channel).

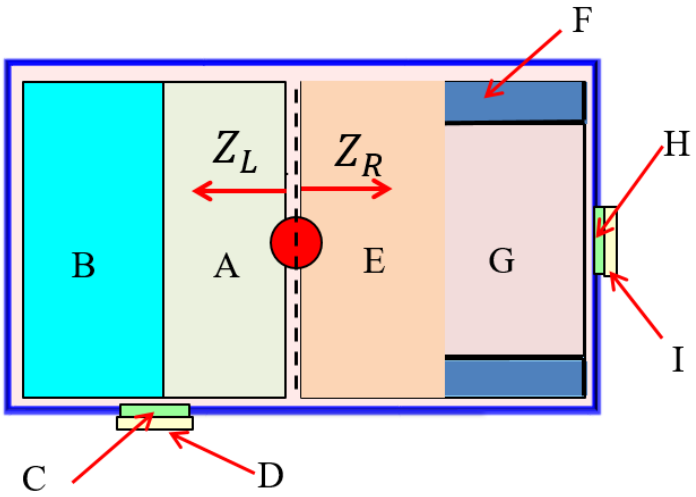

Figure 4.5 Schematic showing plane wave strategy for partial enclosure with quarter wave tube (opening on left side of channel).

Table 4.2 Plane wave model dimensions in longitudinal direction for test case-large quarter wave tube (opening on left side of channel).

Element	Type	Length (cm)	Area (cm^2)
A	Duct	24	2690
B	Quarter Wave Tube	24	2690
C	Duct	1	79
D	Termination Impedance	N/A	79
E	Duct	24.5	2690
F	Quarter Wave Tube	23.5	1006
G	Duct	23.5	1684
H	Duct	1	79
I	Termination Impedance	N/A	79

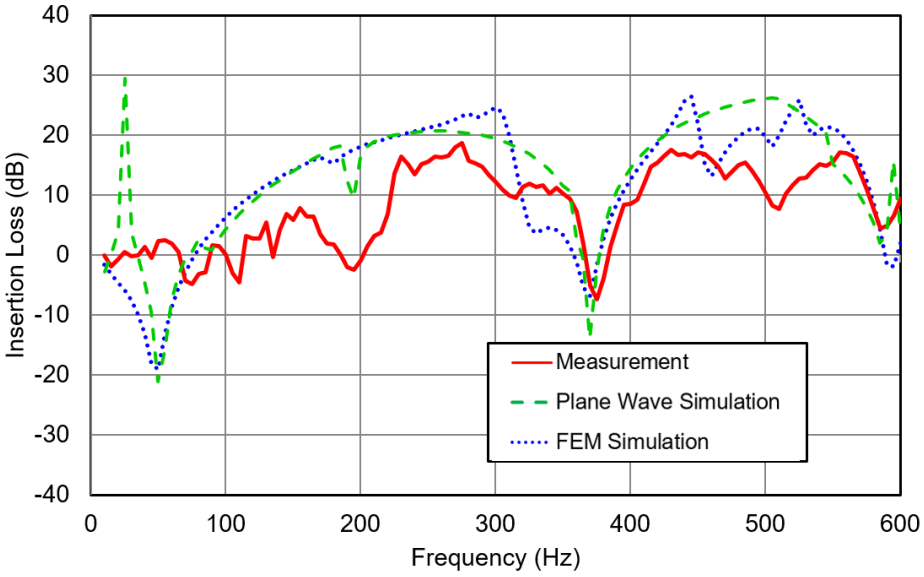

Figure 4.6 Insertion loss comparison for enclosure with quarter wave tube (opening on left side of channel) showing measurement, plane wave simulation, and finite element simulation.

For the third configuration, a quarter wave tube occupying less total volume is considered. The cross-sectional area of the channel is reduced 1006 cm^2 and the center length of the resonator is 27 cm. The channel includes a U-turn which adds additional length to the quarter wave tube as long as plane wave propagation can be assumed. A schematic with dimensions is shown in Figure 4.7. The respective plane wave model is shown in Figure 4.8. Dimensions for the model are summarized in Table 7. Figure 4.9 shows the insertion loss comparison. It can be seen that plane wave simulation identifies that the insertion loss will be improved at 375 Hz though the amount of improvement is over predicted. Nonetheless, the measured insertion loss demonstrated a substantial improvement of approximately 10 dB. This result again demonstrates the usefulness of plane wave simulation to correctly identify the frequency of improvement. However, this should be followed by acoustic FEM analysis to more correctly identify the amount of improvement at the frequency of interest.

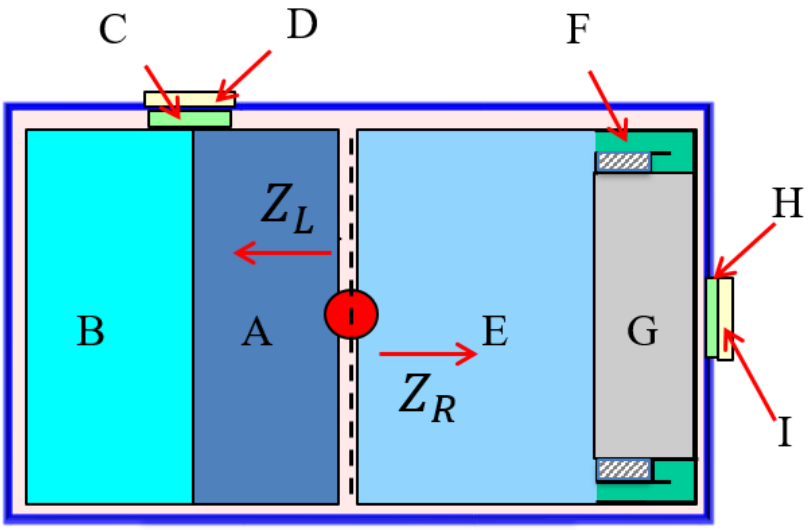

Figure 4.7 Schematic showing plane wave strategy for partial enclosure with quarter wave tube (smaller cross-section U-turn configuration).

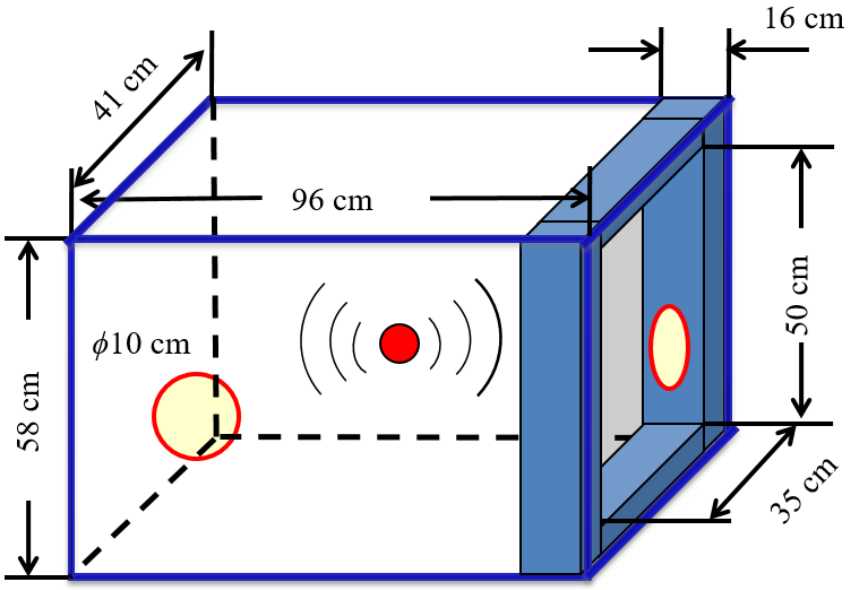

Figure 4.8 Schematic showing partial enclosure with quarter wave tube (smaller cross-section U-turn configuration).

Table 4.3 Plane wave model dimensions in longitudinal direction for test case-small quarter wave tube.

Element	Type	Length (cm)	Area (cm^2)
A	Duct	24	2690
B	Quarter Wave Tube	24	2690
C	Duct	1	79
D	Termination Impedance	N/A	79
E	Duct	32	2690
F	Quarter Wave Tube	23.5	318
G	Duct	16	2372
H	Duct	1	79
I	Termination Impedance	N/A	79

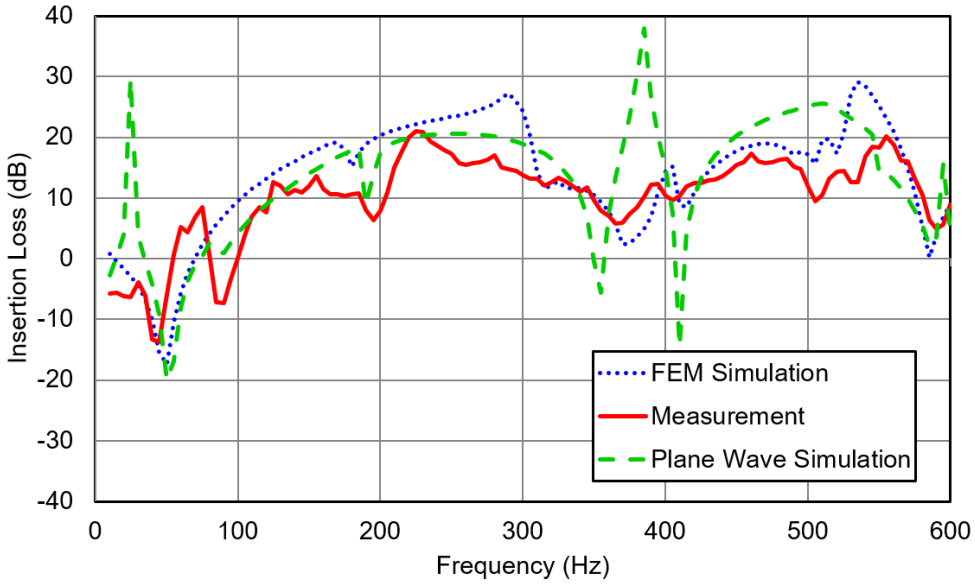

Figure 4.9 Insertion loss comparison for enclosure with quarter wave tube (smaller cross-section U-turn configuration) showing measurement, plane wave simulation, and finite element simulation.

4.2 Helmholtz Resonator

The final case examined is an array of Helmholtz resonators at one end of the enclosure. Eight equal sized Helmholtz resonators were positioned with four on each side of the enclosure. A schematic of the test setup is shown in Figure 4.10. The plane wave model in the lengthwise direction is shown in Figure 4.11, and associated dimensions are detailed in Table 3.8. The resonators are tuned for a frequency of 375 Hz which corresponds with a resonance of the partial enclosure where the insertion loss is adversely affected.

Insertion loss results are shown in Figure 4.12. The plane wave methodology is used and is successful in identifying the frequency of performance improvement though it is less successful at predicting the amount of improvement in dB. The measurement demonstrates that the insertion loss improved by over 20 dB at 375 Hz with the Helmholtz resonators included.

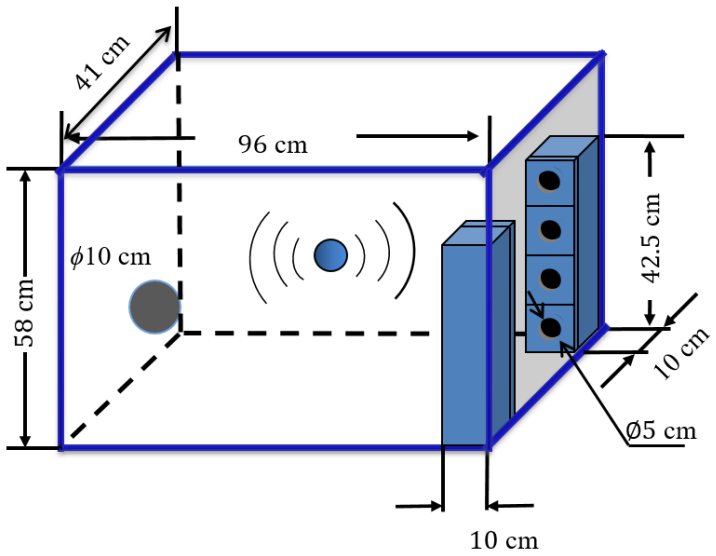

Figure 4.10 Schematic showing partial enclosure with Helmholtz resonator array.

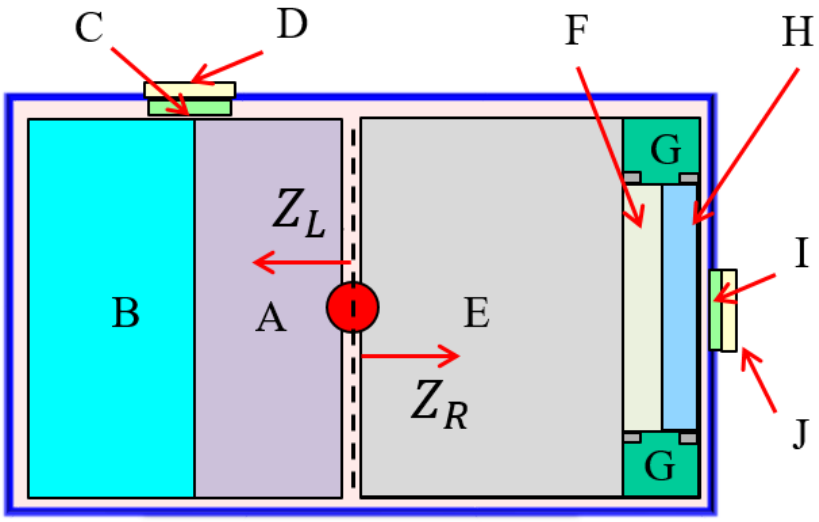

Figure 4.11 Schematic showing plane wave strategy for partial enclosure with Helmholtz resonator array.

Table 4.4 Plane wave model dimensions in longitudinal direction for test case – Helmholtz resonator array.

Element	Type	Length (cm)	Area (cm^2)
A	Duct	24	2690
B	Quarter Wave Tube	24	2690
C	Duct	1	79
D	Termination Impedance	N/A	79
E	Duct	38	2690
F	Duct	5	1840
H	Duct	5	1840
I	Duct	1	79
J	Termination Impedance	N/A	79
Element	Type	Neck Length (cm)	Volume (cm^3)
G	Helmholtz Resonator	1	900

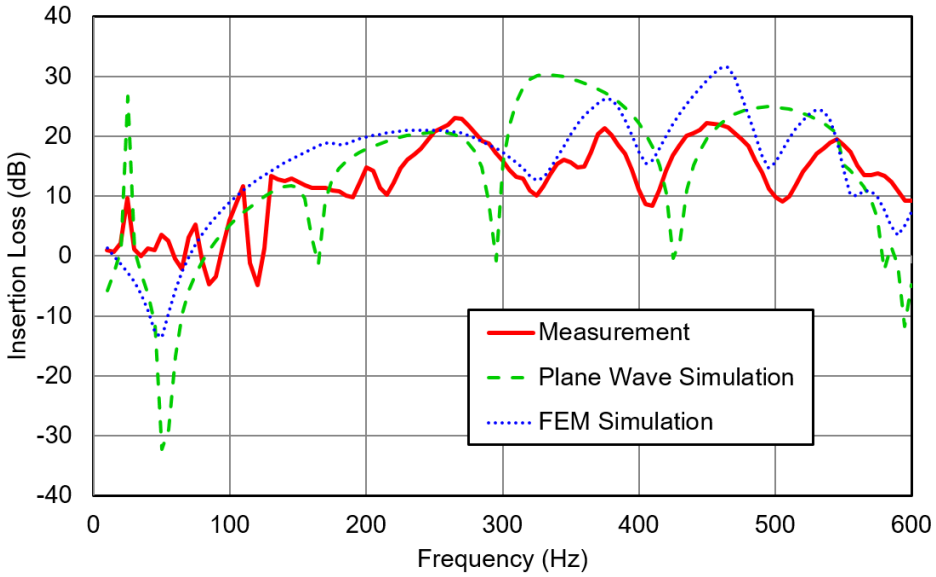

Figure 4.12 Insertion loss comparison for enclosure with Helmholtz resonator array showing measurement, plane wave simulation, and finite element simulation.

These results demonstrate the possible improvements to the insertion loss of partial enclosures that can be gained by inserting reactive elements. Also, it has been demonstrated that these resonators can be tuned and positioned using plane wave simulation. Following that, the amount of improvement can be properly gaged using acoustic FEM simulation.

CHAPTER 5 CONCLUSIONS AND RECOMMENDATIONS FOR FUTURE WORK

5.1 Conclusions

A plane wave simulation approach for determining the insertion loss of partial enclosures at low frequencies was developed. The approach was applied to a partial enclosure with two openings, and then compared to acoustic finite element simulation and direct measurement. It was shown that the first few acoustic modes could be identified for the enclosure. The first few modes are generally the most problematic because they are likely to correspond to engine running frequencies and sound absorption is not very effective. Using simulation, the method was also applied to a large geometry source. It was shown that the procedure could successfully determine the insertion loss with the source geometry included. Though errors might exceed 10 dB at specific frequencies, the method proved useful for identifying design changes that would prove beneficial.

Several design changes were considered for the test enclosure. These included adding quarter wave tubes and Helmholtz resonator arrays. It was shown that the plane wave approach could successfully identify the effect of adding resonators. Moreover, it was demonstrated that adding resonators could improve the enclosure performance by up to approximately 20 dB.

The following are the major contributions of the research. It was demonstrated that:

1. The simple plane wave simulation approach developed could be used to approximately determine the insertion loss of partial enclosures at the lower frequencies. Specifically, the insertion loss trough frequencies can be determined.
2. Resonators like quarter wave tubes and Helmholtz resonators can markedly improve the performance of partial enclosures.
3. Acoustic finite element analysis can be used to determine partial enclosure insertion loss accurately if the automatically matched layer boundary condition is used at the opening.

5.2 Recommendations for Future Work

The following recommendations are suggested. Future work should include:

1. The inclusion of sound absorptive materials into the plane wave model in order to improve the predictions.
2. Determining methods to include structural modal effects into the predictions so as to permit more accurate predictions of the insertion loss at lower frequencies.
3. A more extensive study to assess the impact of acoustic resonators in partial enclosures so that design guidelines can be established.

References

[1] I. L. Ver.,2006. Enclosures, Cabins, and Wrappings, in: I.L. Ver, L.L. Beranek (Eds.), Noise and Vibration Control Engineering, Principles and Applications, Wiley, Hoboken, New Jersey, 517-556.

[2] R. S. Jackson., 1966. “Some Aspects of the Performance of Acoustic Hoods,” Journal of Sound and Vibration 3(1), pp. 82-94.

[3] M. C. Junger., 1970. “Sound Transmission through an Elastic Enclosure Acoustically Coupled to a Noise Source,” ASME Paper No. 70-WA/DE-12.

[4] L. W. Tweed and D. R. Tree., 1978. “Three Methods for Predicting the Insertion Loss of Close Fitting Acoustical Enclosures,” Noise Control Engineering, 10, pp. 74-79.

[5] D. J. Oldham and S. N. Hillarby., 1991. “The Acoustical Performance of Small Close Fitting Enclosures. I. Theoretical Models,” Journal of Sound and Vibration, 150, pp. 261-281.

[6] B. H. Sharp., 1973. “A Study of Techniques to Increase the Sound Insulation of Building Elements.” U.S. Department of Housing and Urban Development, NTIS PB 222 829/4, U.S.A.

[7] F. Sgard, H. Nelisse, N. Atalla, C. K. Amedin, and R. Oddo., 2010. “Prediction of the Acoustical Performance of Enclosures using a Hybrid Statistical Energy Analysis: Image Source Model, Journal of the Acoustical Society of America, 127(2), pp. 784-795.

[8] F. Augusztinovicz, P. Sas, L. Cremers, R. Liebregts., 1996. and M. Mantovani, “Prediction of Insertion Loss of Engine Enclosures by Indirect BEM Calculations, Combined with a Substitution Monopole Source Description Technique”, Proceedings of the International Conference on Noise and Vibration Engineering, Leuven, Belgium, pp. 55-68.

[9] L. Zhou, A. E. Carter, D. W. Herrin, J. Shi, and D. C. Copley., 2011. "Airborne Path Attenuation of Partial Enclosures: Simulation and Sensitivity Study," Applied Acoustics, 72, pp. 380-386.

[10] F. J. Fahy, C. Schofield., 1980. “A Note on the Interaction between a Helmholtz Resonator and an Acoustic Mode of an Enclosure,” Journal of Sound and Vibrations, 72, pp. 365–378.

[11] A. Cummings., 1992. “The Effects of a Resonator Array on the Sound Feld in a Cavity,” Journal of Sound and Vibrations, 154, pp. 25-44.

[12] S. J. Estève and M. E. Johnson., 2002. “Reduction of sound transmission into a circular cylindrical shell using distributed vibration absorbers and Helmholtz resonators,” J. Acoust. Soc. Am., 112, pp. 2840–2848.

[13] G. Yu and L. Cheng., 2009. “Location optimization of a long T-shaped acoustic resonator array in noise control of enclosures,” Journal of Sound and Vibrations, 328, pp. 42–56.

[14] M. L. Munjal., 2014. Acoustics of ducts and mufflers, 2nd ed., West Sussex, UK: John Wiley & Sons

[15] A. D. Pierce., 1981. “Acoustics, An Introduction to Its Physical Principles and Applications,” McGraw-Hill.

[16] H. Levine, J. Schiwinger., 1948. “On the Radiation of Sound from an Unflanged Circular Pipe,” Physical Review, 73:383-406.

[17] J. P. Berenger, “A Perfectly Matched Layer for the Absorption of Electromagnetic Waves,” Journal of Computational Physics, 114(2), pp. 185–200.

[18] C. K. Tam, L. Auriault, and F. Cambuli., 1994. “Perfectly Matched Layer as an Absorbing Boundary Condition for the Linearized Euler Equations in Open and Ducted Domains, Journal of Computational Physics, 144(1), pp. 213–34, 1998.

[19] A. L. Bermudez, L. Hervella-Nieto, A. Prieto, and R. Rodriguez., 2007. “An Optimal Perfectly Matched Layer with Unbounded Absorbing Function for Time-Harmonic Acoustic Scattering Problems,” Journal of Computational Physics, 223(2), pp. 469–488.

[20] D. Casalino and M. Genito., 2008. “Achievements in the Numerical Modeling of Fan Noise Radiation from Aeroengines,” Aerospace Science and Technology 12(1), pp. 105–113.

[21] Siemens., 2017. LMS Virtual.Lab Online Help. Munich, Germany: Siemens Product Lifecycle Management Software Inc.

[22] ANSYS Academic Research., 2016. Release 16.2.

[23] D. W. Herrin, X. Hua, Y. Zhang, and T. Elnady., 2014. “The Proper Use of Plane Wave Models for Muffler Design,” SAE International Journal of Passenger Cars – Mechanical Systems, Vol. 7, No. 3.

VITA

Shujian He was born in Gaoqing, China in 1990. He graduated from Zibo Experimental High School in 2008. He received the degree of Bachelor of Science in Mechanical Engineering from University of Kentucky in May, 2013. He received the degree of Bachelor in Mechanical Engineering and Automation from China University of Mining and Technology in July, 2013. In August, 2013, he enrolled in the Department of Mechanical Engineering, University of Kentucky. During the four years' studies at University of Kentucky, He published two Noise-Con conference papers as first author and one Inter-Noise paper as second author. The fourth paper has been done and submitted to NCEJ.

Shujian He